Supporting information

A novel Bismuth hydroxide ($Bi(OH)_3$) semiconductor with efficient photocatalytic activity†

Sitong Liu[a], Guangmin Ren[a], Xinyu Gao[a] , Zizhen Li[a], Liang Wang[a] and Xiangchao Meng[a, *]

a Key Laboratory of Marine Chemistry Theory and Technology, Ministry of Education, College of Chemistry and Chemical Engineering, Ocean University of China, Qingdao, 266100, China.

*Corresponding Author: mengxiangchao@ouc.edu.cn

Number of pages: 27

Number of figures: 17

Number of Tables: 2

Table of Contents

S1. Experimental part

S1.1. Preparation of $Bi(OH)_3$

The $Bi(OH)_3$ were successfully synthesized through a simple one-step hydrothermal method. In a typical process, 1 mmol $Bi(NO_3)_3 \cdot 5H_2O$ was dispersed in 30 mL deionized water under ultrasonication. Then, the pH of the suspension was adjusted to 4, 7, 10, 12 and 14 by adding 10 M KOH. After stirring for 1 h at ambient temperature, the suspension was transferred into 100 mL Teflon-lined stainless-steel autoclaves and maintained at 150 °C for 12 h. The white precipitate was collected by centrifugation, rinsed thoroughly with deionized water, and dried at 80 °C for 12 h.

S1.2. Characterization

X-ray diffraction (XRD) patterns were recorded on an Ultima IV X-ray diffraction with Cu-Kα radiation. Scanning electron microscopy (SEM) was performed with a Thermo Scientific ESCALAB Xi+ system. Ultraviolet-visible (UV–vis) diffuse reflectance spectra (DRS) of samples and the absorption spectra of phenol were analyzed by a Hitachi UV-3150 spectrometer. The elemental composition of samples was carried out using X-ray photoelectron spectra (XPS) on a Thermo Scientific ESCALAB Xi+ system with Mono AlKa radiation ($h\upsilon$ = 1486.6 eV). Thermogravimetric (TG) measurements were carried out on STA6000 Thermogravimetry Analyzer. The CO_2 adsorption capacity of the catalysts was determined by by temperature-programmed desorption of CO_2-TPD (AutoChem1 II 2920). Before TPD experiments, the samples were plugged with helium at 250 °C for 60 min in order to remove any contaminations.

After cleaning, the samples were cooled and saturated for 20 min in flow of pure at 50 °C. Then, the samples were purged in helium flow until a constant baseline level was attained. TPD measurements were performed from 50 °C to 300 °C at a rate of 10 °C/min using helium as carrier flow. The evolved CO_2 were detected by an on-line TCD calibrated by the peak area of known pulses of CO_2. The TOC change was analyzed by a Shimadu TOC-L. The CO_2 adsorption capacity of the catalysts was determined by by temperature-programmed desorption of CO_2-TPD (AutoChem1 II 2920). Before TPD experiments, the samples were plugged with helium at 250 °C for 60 min in order to remove any contaminations. After cleaning, the samples were cooled and saturated for 20 min in flow of pure at 50 °C. Then, the samples were purged in helium flow until a constant baseline level was attained. TPD measurements were performed under 300 °C at a rate of 10 °C/min using helium as carrier flow. The evolved CO_2 were detected by an on-line TCD calibrated by the peak area of known pulses of CO_2.

S1.3. Photocatalytic CO_2 conversion

Photocatalytic reactions were conducted in a closed circulating system (CEL-SPH2N-D9, Beijing China Education Au-Light Co., Ltd.) irradiated with a 300 W Xenon lamp. Herein, 20 mg of catalyst was uniformly dispersed in 50-mL deionized water in the quartz glass reactor. Then, the photoreactor system needed a thorough vacuum treatment, and CO_2 gas of high purity introduced into the circulation system. During 6 h of reaction, the amount of product was analyzed using on-line gas chromatography (GC-7920, Beijing China Education Au-Light Co., Ltd.) equipped with an FID detector.

S1.4 Photocatalytic degradation

The degradation activity was evaluated by measuring the degradation of phenol. 50 mg (0.5 g/L) catalyst was added into 100 mL aqueous solution of 10 mg/L of phenol, RhB and MB. After stirring for 30 min in the dark to obtain an adsorption-desorption equilibrium, the system was tested under 300 W Xenon light. Aliquots were drawn and analyzed using a UV–vis spectrometer (Hitachi UV-3150 spectrometer) at the maximum absorption wavelength (269 nm of phenol, 554 nm of RhB and 664 nm of MB) at every certain minute after centrifuging.

S1.5 Photocatalytic H_2 production reaction

For photocatalytic H_2 production, 50 mg of $Bi(OH)_3$ catalyst was dispersed in 90 mL deionized water and 10 mL methanol. Evacuation of the reaction system to remove other gases. A 300 W Xe lamp was used as light source (Perfect Light, Beijing). The collected gaseous products were detected by GC using a thermal conductivity detector (TCD).

S1.6 Electrochemical measurements

The photoelectrochemical measurements were carried out in a three-electrode cell on CHI 660E electrochemical workstation. A saturated calomel electrode and platinum electrode were used as the reference electrode and the counter electrode, respectively. FTO conductive glasses coated with prepared samples were usedas working electrode. Specifically: samples (5 mg) were dissolved in ethylene glycol (100 μL) with Nafion 117 solution (50 μL) and ultrasonically dispersed to form a homogeneous suspension,

then it was drop-coated to the FTO conductive glass with the area of 1×1 cm^2 and airing dried it.

The electrochemical impedance spectra (EIS) were tested at the frequency varied between 105 to 0.1 Hz with 5 mV amplitude. The ON-OFF photo-induced transient current was measured at a bias voltage of 0.4 V, irradiated by 300 W Xe lamp.

S2. Results

S2.1 XRD patterns

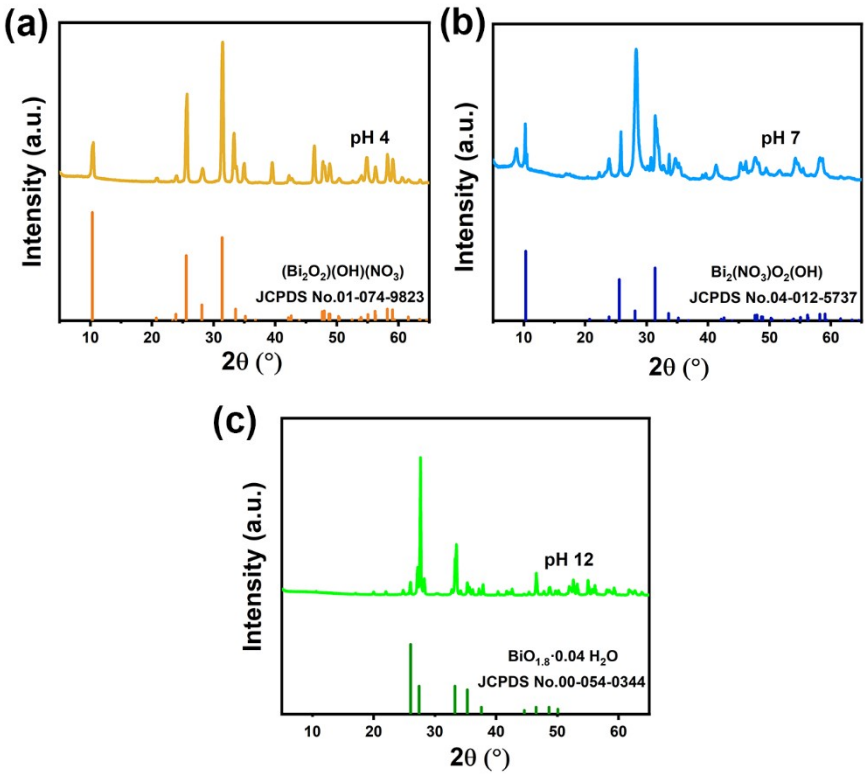

Fig. S1 XRD patterns of sample at pH 4, pH 7 and pH 12.

S2.2 SEM and XRD spectra

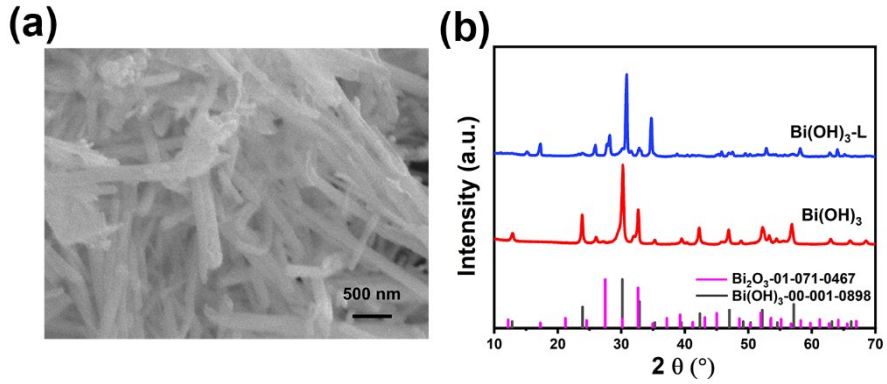

Fig. S2 (a) SEM image and (b) XRD patterns of $Bi(OH)_3$ after illumination.

S2.3 EPR spectra

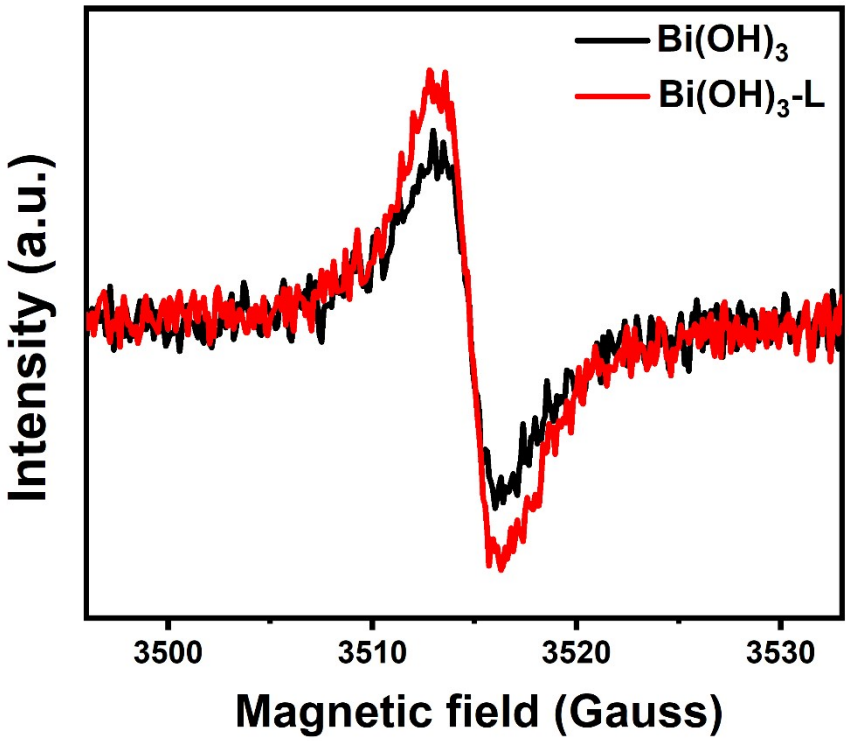

Fig. S3 EPR spectra of $Bi(OH)_3$ before and after illumination.

S2.4 DRS spectra

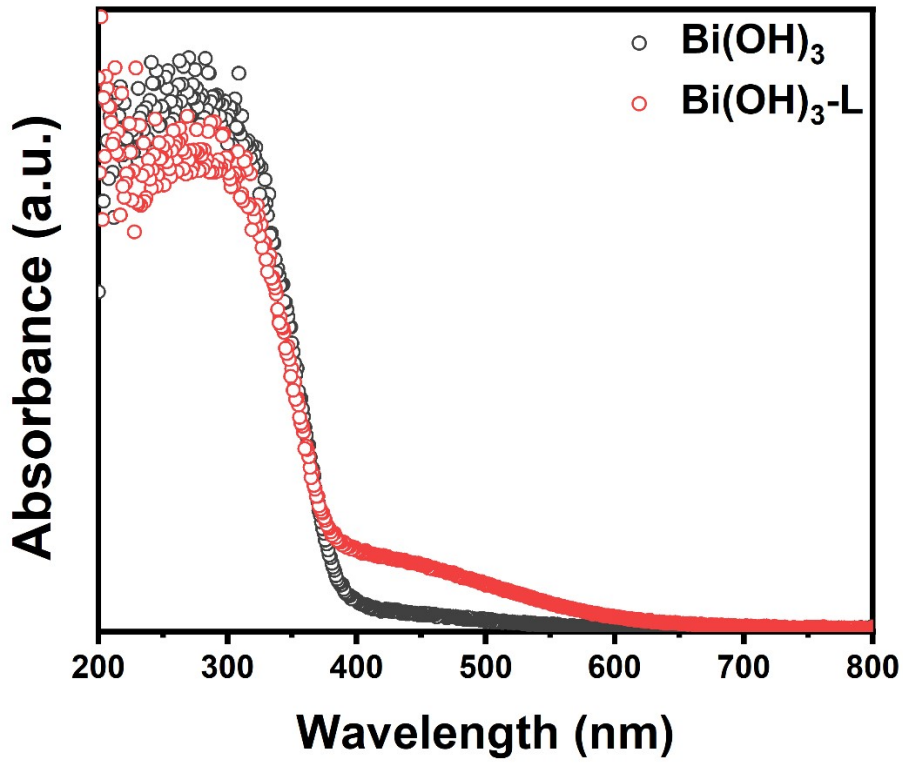

Fig. S4 UV-vis DRS spectra of $Bi(OH)_3$ before and after illumination ($Bi(OH)_3$-L).

S2.5 Tauc plots and VB-XPS spectra

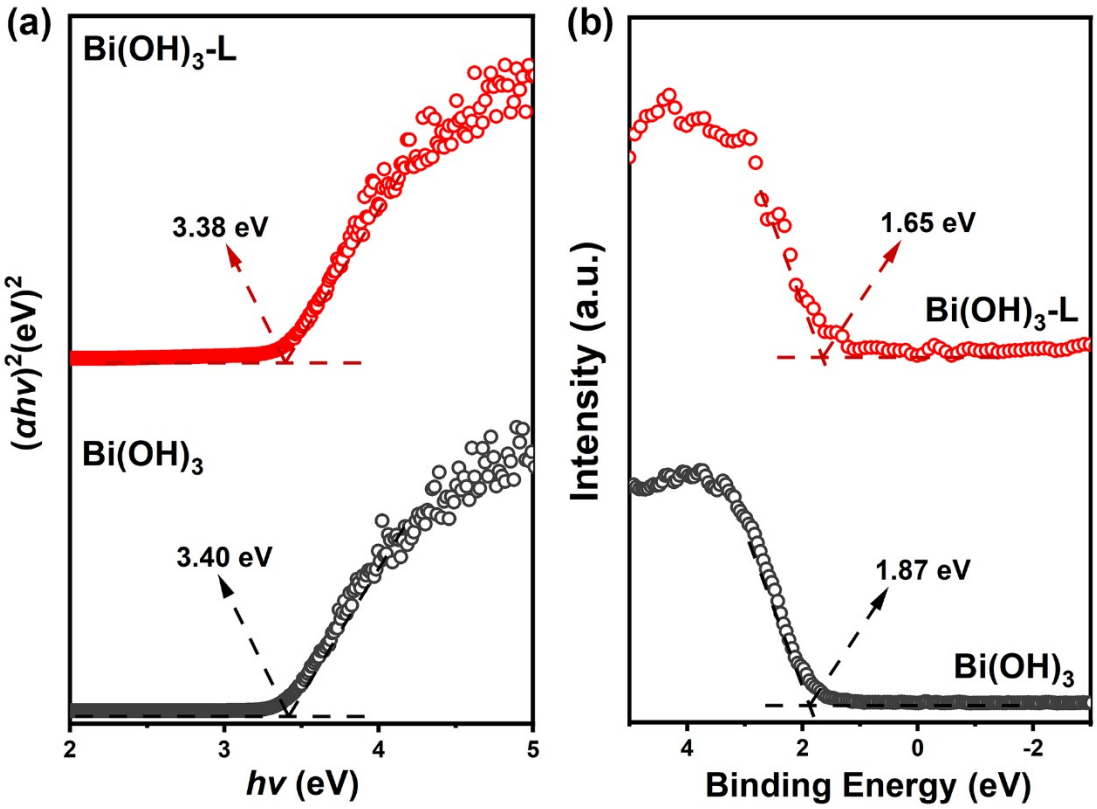

Fig. S5 (a) Tauc plots and (b) VB-XPS spectra of $Bi(OH)_3$ before and after illumination.

S2.6 Photocurrent response

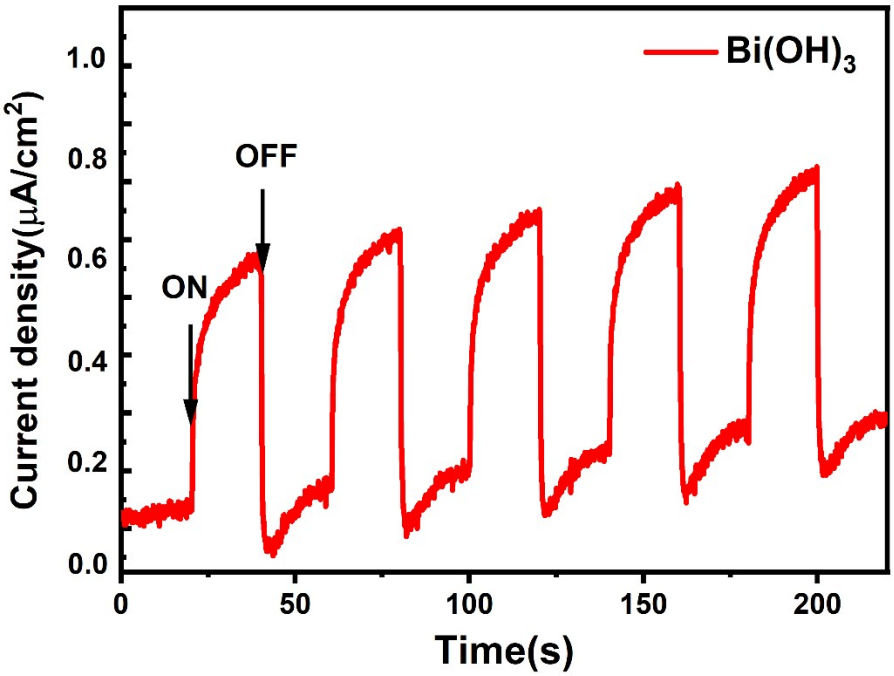

Fig. S6 Photocurrent response of $Bi(OH)_3$.

S2.7 Thermal Stability

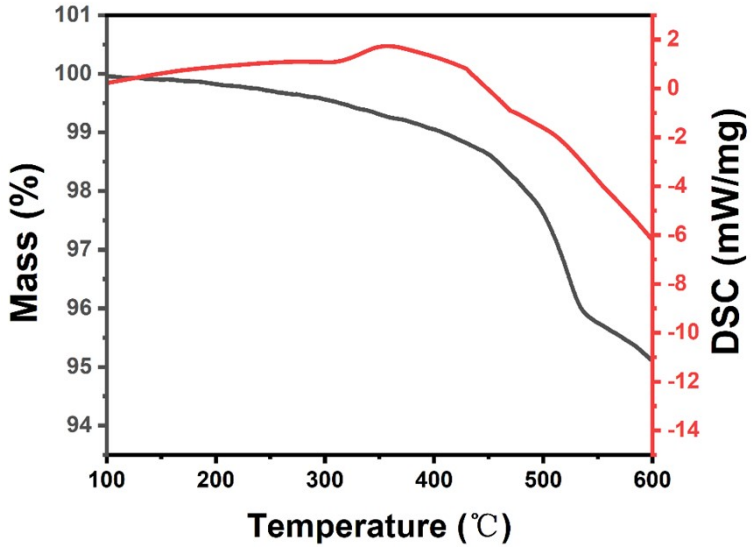

Fig. S7 Thermogravimetric (TG) curve of $Bi(OH)_3$ under air atmosphere.

S2.8 Control experiments

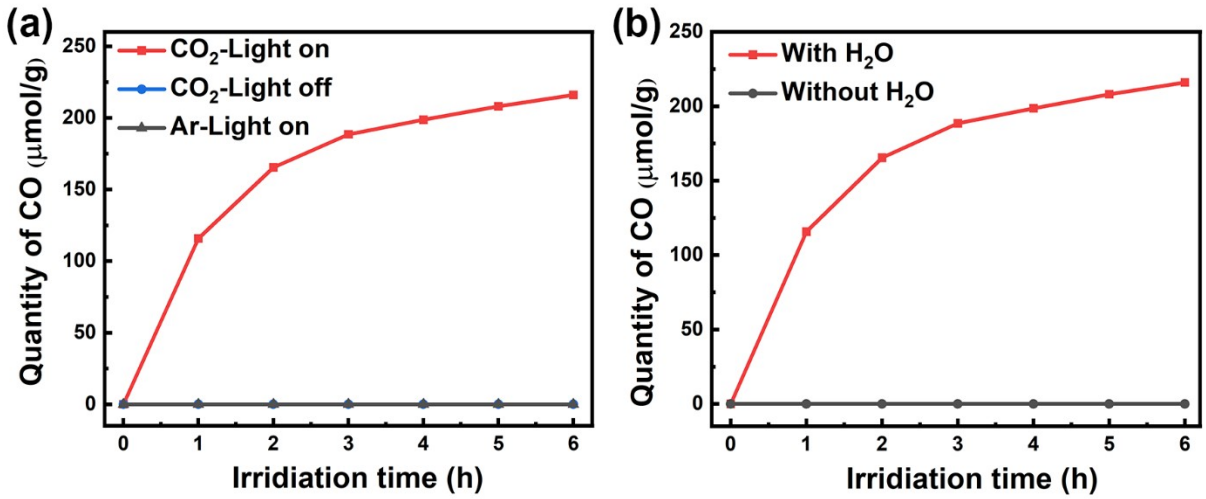

Fig. S8 Photoreduction of CO_2 into CO over $Bi(OH)_3$ under different conditions: (a) with and without light irradiation under CO_2/H_2O and under Ar/H_2O vapor flow and light irradiation; (b) with and without H_2O in CO_2 atmosphere under light irradiation.

S2.9 MS spectra of $^{13}CO_2$

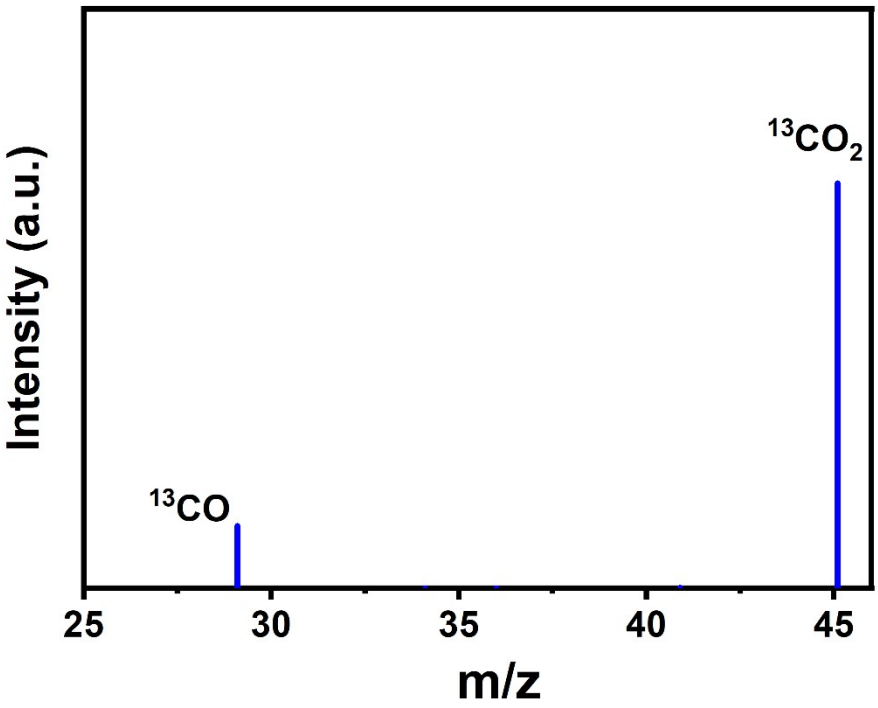

Fig. S9 MS analysis for CO produced from $^{13}CO_2$ isotope experiment.

S2.10 H_2 production

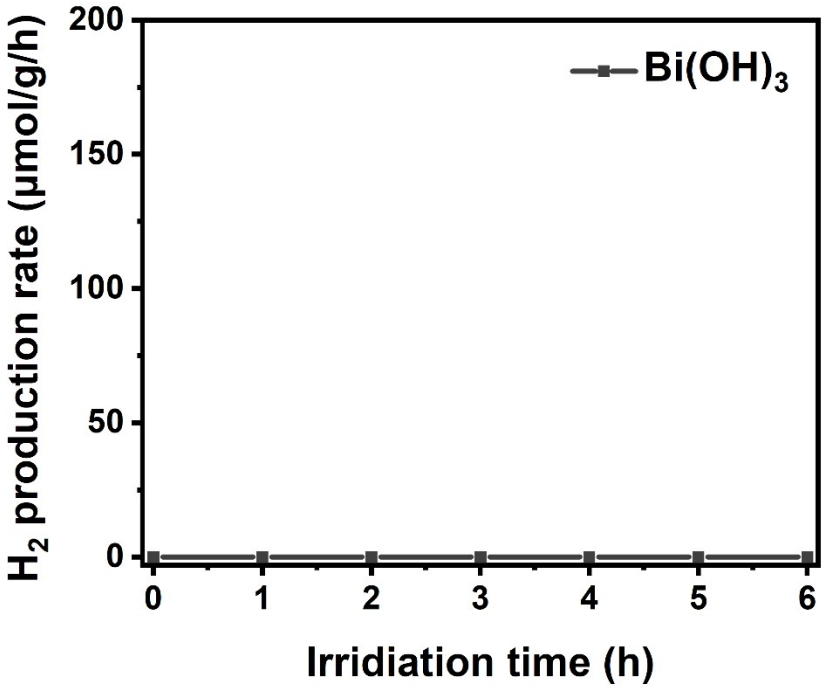

Fig. S10 Photocatalytic H_2 yields of $Bi(OH)_3$.

S2.11 CO_2 photoreduction of Bi_2O_3

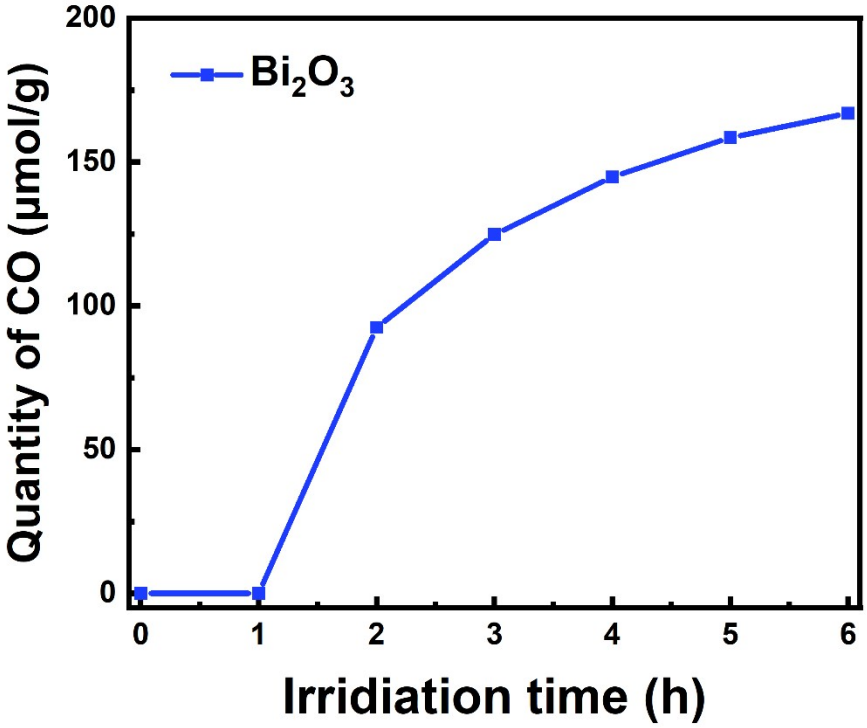

Fig. S11 Photocatalytic CO yields of Bi_2O_3.

S2.12 CO_2-TPD

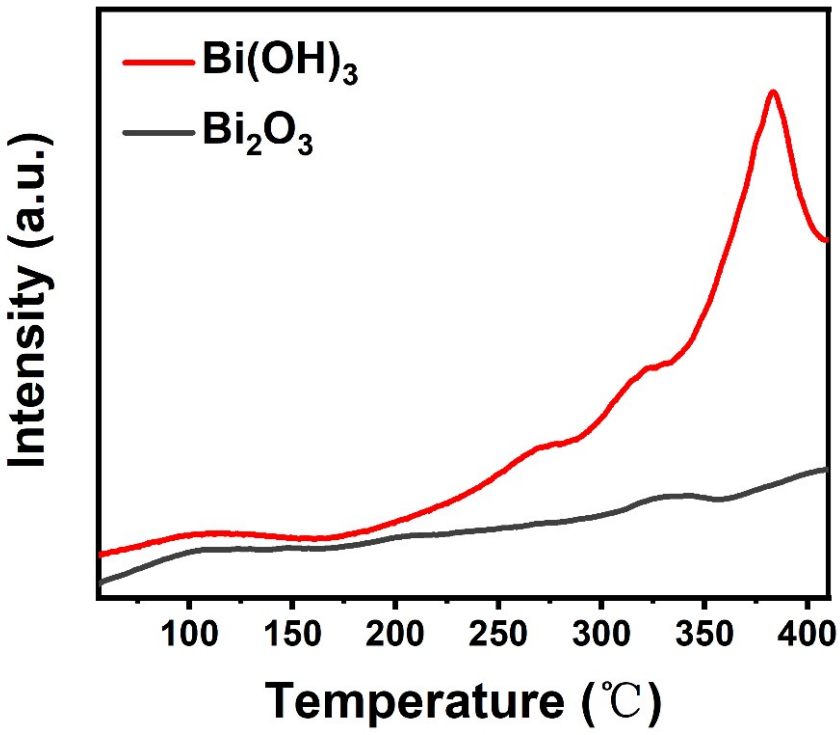

Fig. S12 CO_2-TPD of $Bi(OH)_3$ and Bi_2O_3.

S2.13 TOC removal

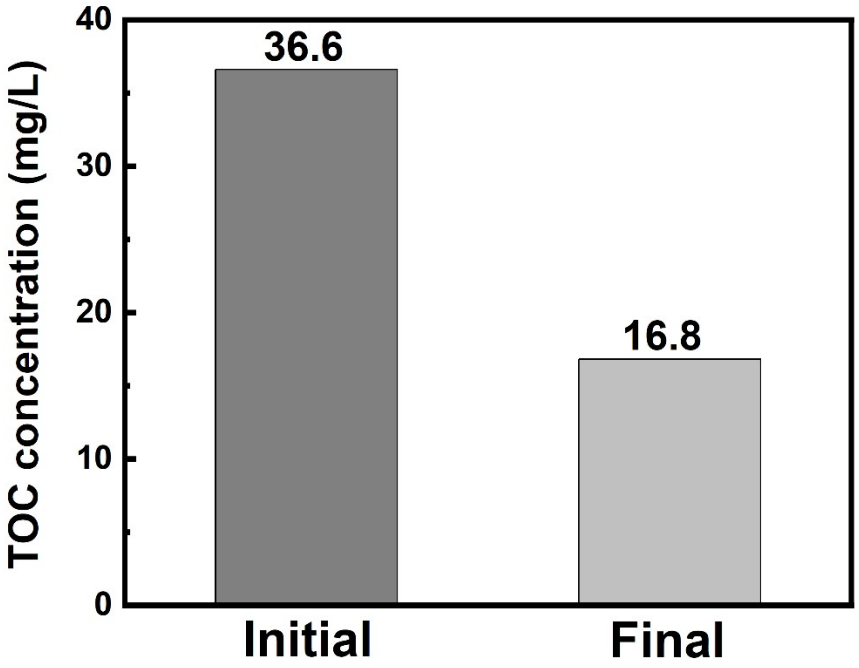

Fig. S13 TOC change in photodegradation 10 mg/L phenol over $Bi(OH)_3$ (catalyst dosage: 0.5g/L).

S2.14 Phenol degradation of Bi_2O_3

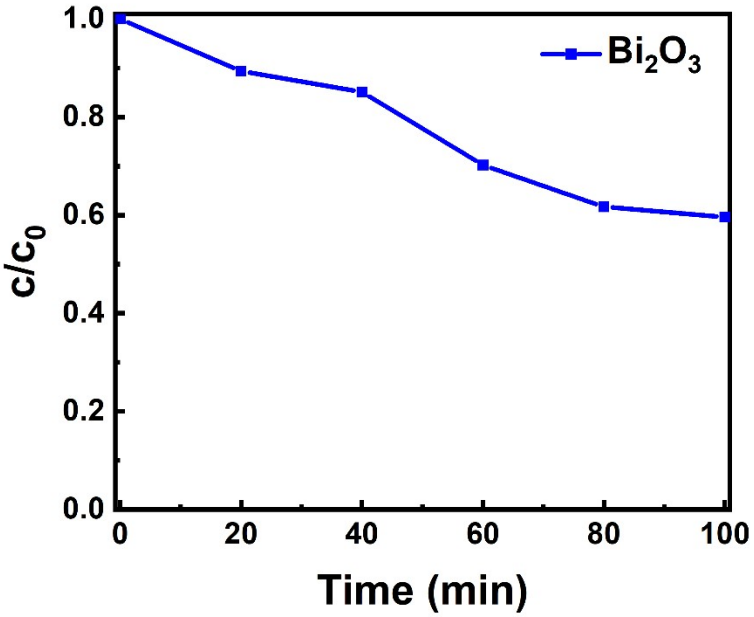

Fig. S14. Photodegradation of 10 mg/L phenol over Bi_2O_3.

S2.15 Photodegradation of dyes

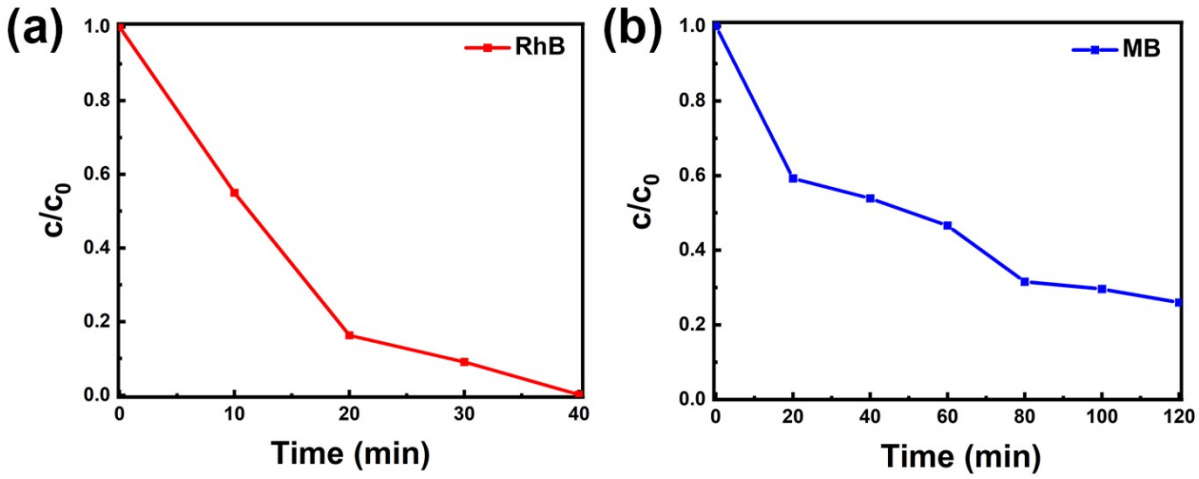

Fig. S15 Photodegradation of 10 mg/L (a) RhB and (b) MB under 300 W Xe lamp.

S2.16 Zeta potential

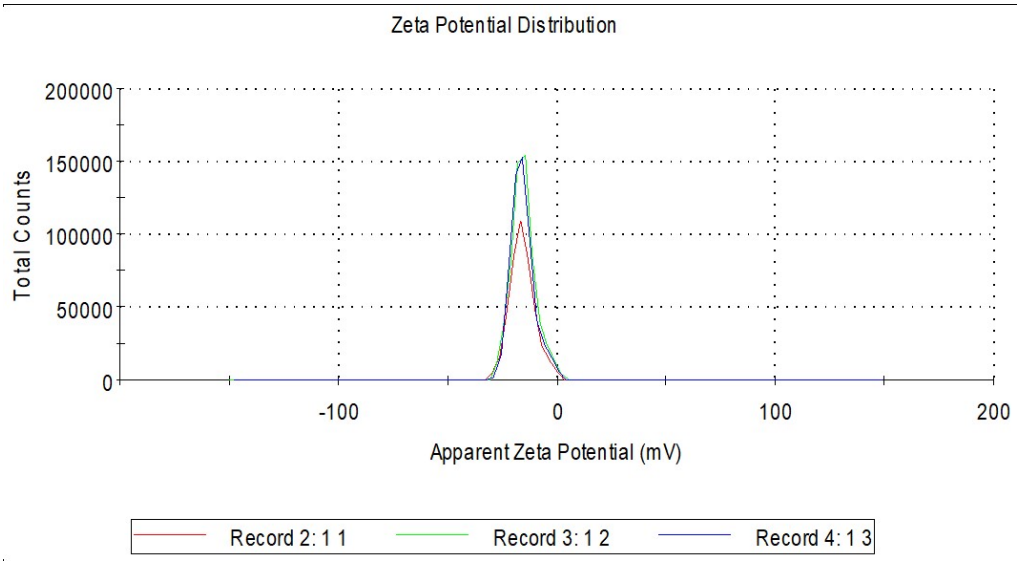

Fig. S16 Zeta potential of $Bi(OH)_3$.

S2.17 Radical species

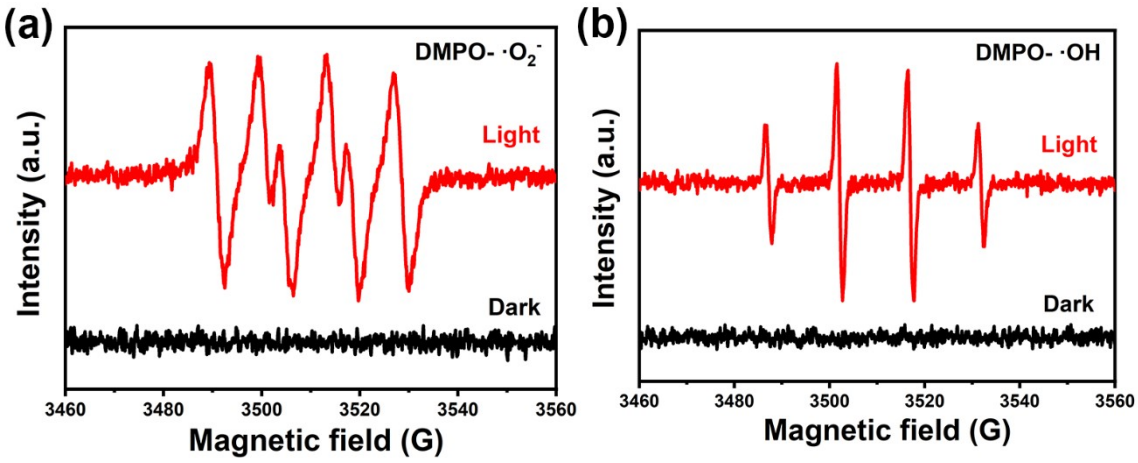

Fig. S17 ESR spectra of radical species trapped by 5, 5-dimethyl-1-pyrroline-N-oxide (DMPO) after 10 min light irradiation with (c) methanol and (d) aqueous dispersion.

S2.18 Comparable table of photocatalytic performance

Table S1 Summary of photocatalysts for CO_2 reduction

Catalyst	Light source	Activity (μmol g^{-1} h^{-1})	Ref.
$Bi(OH)_3$	**300 W Xe lamp**	**CO: 36**	**This work**
TiO_2@CTF-Py	300 W Xe lamp ($\lambda > 320$ nm)	CO: 43.34	[1]
CNFs/TiO_2 NCs	Simulated sunlight	CO: 0.4	[2]
ZnO	300 W Xe lamp	CO: 0.75 CH_4: 0.04	[3]
ZnO/graphene	300 W Xe lamp	CO: 3.38 CH_3OH: 0.59	[4]
OVs-Rich BiOBr Atomic Layers	300 W Xe lamp	CO: 2.03	[5]
g-C_3N_4/BiOCl	300 W Xe lamp	CO: 28.4 CH_4: 4.6	[6]
Bi_2O_{3-x}	940 nm LED light	CO: 4.6	[7]
Bi_2O_3 Nanosheet/Bi_2WO_6	300 W Xe lamp ($\lambda > 400$ nm)	CO: 17.39	[8]
3D Bi_2MoO_6 microspheres	300 W Xe lamp	CO: 41.5	[9]
Bi_2MoO_6 nanosheets	300 W Xe lamp	CO: 14.38	[10]
Zn-Al layered double hydroxides	500 W Xe lamp	CO: 0.62	[11]
Ag_3PO_4/g-C_3N_4	500 W Xe lamp	CO: 39.8 CH_3OH: 8.8	[12]
g-C_3N_4/$Bi_4O_5I_2$	300 W Xe lamp ($\lambda > 400$ nm)	CO: 39.8 CH_3OH: 8.8 CO: 45.6 CH_4: 5.6	[13]
g-C_3N_4/BiOBr	300 W Xe lamp ($\lambda>380$ nm)	CO: 6.67 CH_4: 0.92	[14]
Bi_2WO_6/RGO/g-C_3N_4	300 W Xe lamp ($\lambda>420$ nm)	CO: 16 CH_4: 2.5	[15]
P-doped g-C_3N_4	Simulated sunlight	CO: 2.37	[16]

	(300 W Xe)		
O and C codoped g-C_3N_4	300 W Xe lamp (λ > 420 nm)	CO: 4.6	[17]
In_2O_3	Visible light (λ>420 nm)	CO: 63.3	[18]

Table S2 Summary of photocatalysts for organic pollutions degradation

Catalyst	Light source	Initial concentration	Degradation activities	Degradation Time	Ref.
$Bi(OH)_3$	**300 W Xe lamp**	**Phenol (10 mg/L) RhB (10 mg/L)**	**92.7% 100%**	**180 min 40 min**	**This work**
Pt/TiO_2	High pressure mercury lamp	Phenol (0.43 mM)	~92%	90 min	[19]
Tm-modified TiO_2	Visible light (λ > 420 nm)	Phenol (0.21 mM)	~86%	60 min	[20]
BiOBr/Bismuth Oxyhydrate	UV-vis light	RhB (15 ppm)	100%	50 min	[21]
Pd/Bi_2MoO_6	Visible light	RhB (1×10^{-5} M)	97.35%	150 min	[22]
Ag_2O/Bi_2MoO_6	Visible light (λ > 420 nm)	RhB (10 mg/L)	95%	60 min	[23]
ZnO/ZnMgAl-CO_3-LDHs	12 W UV lamp (λ= 254 nm)	Phenol (10 mg/L)	98%	3 h	[24]
CeO_2/Mg-Al LDH	UV light	Phenol (0.85 mM)	50%	7 h	[25]
Pd-BiOBr	Visible light	Phenol (10 mg/L)	95.1%	180 min	[26]
Carbon quantum dots/BiOBr	300 W Xe lamp (λ > 420 nm)	RhB (10 mg/L)	50%	50 min	[27]
Bi_2O_3@BiOI@ UiO-66	Visible light	RhB (10 mg/L)	89.9%	60 min	[28]
$FeOOH/Bi_2O_3$	300 W Xe lamp	Phenol (20 mg/L)	85%	160 min	[29]

S4. References

1. Z. Xu, Y. Cui, D. J. Young, J. Wang, H.-Y. Li, G.-Q. Bian and H.-X. Li, *Journal of CO_2 Utilization*, 2021, **49**, 101561.
2. Z. Lei, Z. Xiong, Y. Wang, Y. Chen, D. Cao, Y. Zhao, J. Zhang and C. Zheng, *Catalysis Communications*, 2018, **108**, 27-32.
3. P. Li, H. Hu, G. Luo, S. Zhu, L. Guo, P. Qu, Q. Shen and T. He, *ACS Applied Materials & Interfaces*, 2020, **12**, 56039-56048.
4. L. Wang, H. Tan, L. Zhang, B. Cheng and J. Yu, *Chemical Engineering Journal*, 2021, **411**, 128501.
5. L. Wang, G. Liu, B. Wang, X. Chen, C. Wang, Z. Lin, J. Xia and H. Li, *Solar RRL*, 2021, **5**, 2000480.
6. Y. Chen, F. Wang, Y. Cao, F. Zhang, Y. Zou, Z. Huang, L. Ye and Y. Zhou, *ACS Applied Energy Materials*, 2020, **3**, 4610-4618.
7. Y. Li, M. Wen, Y. Wang, G. Tian, C. Wang and J. Zhao, *Angewandte Chemie*, 2021, **133**, 923-929.
8. Z. Xie, Y. Xu, D. Li, S. Meng, M. Chen and D. Jiang, *ACS Applied Energy Materials*, 2020, **3**, 12194-12203.
9. X. Zhang, G. Ren, C. Zhang, R. Li, Q. Zhao and C. Fan, *Catalysis Letters*, 2020, **150**, 2510-2516.
10. S. Li, L. Bai, N. Ji, S. Yu, S. Lin, N. Tian and H. Huang, *Journal of Materials Chemistry A*, 2020, **8**, 9268-9277.
11. N. Ahmed, Y. Shibata, T. Taniguchi and Y. Izumi, *Journal of Catalysis*, 2011, **279**, 123-135.
12. Y. He, L. Zhang, B. Teng and M. Fan, *Environmental Science & Technology*, 2015, **49**, 649-656.
13. Y. Bai, L. Ye, L. Wang, X. Shi, P. Wang, W. Bai and P. K. Wong, *Applied Catalysis B: Environmental*, 2016, **194**, 98-104.
14. Y. Bai, T. Chen, P. Wang, L. Wang, L. Ye, X. Shi and W. Bai, *Sol. Energy Mater. Sol. Cells*, 2016, **157**, 406-414.
15. W.-K. Jo, S. Kumar, S. Eslava and S. Tonda, *Applied Catalysis B: Environmental*, 2018, **239**, 586-598.
16. B. Liu, L. Ye, R. Wang, J. Yang, Y. Zhang, R. Guan, L. Tian and X. Chen, *ACS applied materials & interfaces*, 2018, **10**, 4001-4009.
17. S. Wan, M. Ou, X. Wang, Y. Wang, Y. Zeng, J. Ding, S. Zhang and Q. Zhong, *Dalton Transactions*, 2019, **48**, 12070-12079.
18. X. Zhu, J. Yang, X. Zhu, J. Yuan, M. Zhou, X. She, Q. Yu, Y. Song, Y. She, Y. Hua, H. Li and H. Xu, *Chemical Engineering Journal*, 2021, **422**, 129888.
19. Y. Wang, J. Zhao, X. Xiong, S. Liu and Y. Xu, *Applied Catalysis B: Environmental*, 2019, **258**, 117903.
20. P. Mazierski, P. N. Arellano Caicedo, T. Grzyb, A. Mikolajczyk, J. K. Roy, E. Wyrzykowska, Z. Wei, E. Kowalska, T. Puzyn, A. Zaleska-Medynska and J. Nadolna, *Applied Catalysis B: Environmental*, 2019, **252**, 138-151.

21. S. Shenawi-Khalil, V. Uvarov, S. Fronton, I. Popov and Y. Sasson, *The Journal of Physical Chemistry C*, 2012, **116**, 11004-11012.

22. A. Phuruangrat, T. Klangnoi, P. Patiphatpanya, P. Dumrongrojthanath, S. Thongtem and T. Thongtem, *J. Electron. Mater.*, 2020, **49**, 3684-3691.

23. J. Zhang, H. Liu and Z. Ma, *Journal of Molecular Catalysis A: Chemical*, 2016, **424**, 37-44.

24. S.-Z. Wu, N. Li and W.-D. Zhang, *J. Porous Mater.*, 2014, **21**, 157-164.

25. J. S. Valente, F. Tzompantzi and J. Prince, *Applied Catalysis B: Environmental*, 2011, **102**, 276-285.

26. X. Meng, Z. Li and Z. Zhang, *Materials Research Bulletin*, 2018, **99**, 471-478.

27. J. Xia, J. Di, H. Li, H. Xu, H. Li and S. Guo, *Applied Catalysis B: Environmental*, 2016, **181**, 260-269.

28. J. Tang, T. Zhang, Z. Duan, C. Li, C. Meng, Y. Zhang, Q. Zhang, D. Hou, Q. Xv and Y. Zhu, *Chem. Phys. Lett.*, 2021, **768**, 138354.

29. D. He, X. Wu, Y. Chen, Y. Situ, L. Zhong and H. Huang, *Chemosphere*, 2018, **210**, 334-340.